

Diagnostic utility of neuroretinal rim thickness, measured in clock-hour sectors with HD optical coherence tomography, in preperimetric glaucoma

Tzu-Yang Tai^a, Yu-Chieh Ko^{a,b}, Yu-Fan Chang^{a,c}, Catherine Jui-Ling Liu^{a,b}, Mei-Ju Chen^{a,b,*}

^aDepartment of Ophthalmology, Taipei Veterans General Hospital, Taipei, Taiwan, ROC; ^bDepartment of Ophthalmology, Faculty of Medicine, School of Medicine, National Yang-Ming University, Taipei, Taiwan, ROC; ^cInstitute of Clinical Medicine, National Yang-Ming University, Taipei, Taiwan, ROC

Abstract

Background: We evaluated the usefulness of neuroretinal rim (NRR) thicknesses, measured in clock-hour sectors with Cirrus HD optical coherence tomography, for diagnosing preperimetric glaucoma (PPG).

Methods: This prospective study included 39 eyes of 39 patients with PPG and 39 eyes of 39 controls that were matched to patients for age and refractive error. We measured the circumpapillary retinal nerve fiber layer (cpRNFL) thickness, macular ganglion cell-inner plexiform layer (GCIPL) thickness, and optic nerve head (ONH) parameters with optical coherence tomography. The clock-hour NRR thicknesses were derived from a 360° circumferential rim thickness curve. We analyzed the area under the receiver operating characteristics curve (AUROC), cutoff values, and sensitivities at specificities of 90% and 95%.

Results: The largest area under the receiver operating characteristics curves were observed for the NRR thickness at 6 o'clock (0.823), the inferior RNFL thickness (0.821), the average RNFL thickness (0.819), and the NRR thickness at 7 o'clock (0.818). The performance of the NRR thickness at 6 o'clock was comparable to the best performances of the cpRNFL, GCIPL, and ONH parameters (all $p > 0.05$).

Conclusion: The ability of the clock-hour NRR thickness assessment to diagnose PPG was comparable to the diagnostic abilities of cpRNFL, GCIPL, and ONH parameters. The best indicator of PPG was the NRR thickness parameter that was at 6 o'clock. This finding could play a role in detecting early structural changes in PPG.

Keywords: Glaucoma; Optical coherence; Refractive error.

1. INTRODUCTION

Glaucoma is an optic neuropathy characterized by changes in the optic nerve head (ONH) and retinal nerve fiber layer (RNFL) with associated visual field (VF) defects. Glaucomatous ONH changes include enlargement of the cup-to-disc ratio (CDR) and thinning and notching of the neuroretinal rim (NRR). Preperimetric glaucoma (PPG) is characterized by a glaucomatous optic disc, abnormal RNFL, and normal VF. Early detection of structural changes associated with retinal ganglion cell loss is particularly important in PPG.

The reproducible, successful evaluation of the ONH was facilitated with the introduction of spectral-domain optical coherence tomography (OCT). The built-in ONH analysis algorithm of the Cirrus HD spectral-domain OCT (Cirrus HD-OCT; Carl Zeiss

Meditec, Dublin, CA) automatically identifies the optic disc margin, at the termination of Bruch's membrane, and the cup borders. The software then measures the neuroretinal tissue between the optic disc margin and the cup margin around the entire circumference of the ONH. Based on these measurements, the NRR width (thicknesses) is determined automatically.¹ Previous studies that employed the Cirrus HD-OCT reported good reproducibility in measuring the average rim areas and the ability of those measurements to diagnose early glaucoma and PPG.¹⁻³

Sectorial NRR assessments in early glaucoma were studied,⁴ but no study has been investigated in patients with PPG yet. Therefore, we aimed to evaluate the ability of different clock-hour NRR thicknesses in diagnosing PPG. The NRR thicknesses at different clock-hour locations were derived from a 360° circumferential rim thickness curve obtained with the Cirrus HD-OCT. Then, the clock-hour thicknesses that showed the best diagnostic ability were compared to traditional OCT parameters for diagnosing patients with PPG.

2. METHODS

Patients with PPG who visited the outpatient clinic of Taipei Veterans General Hospital between January 2017 and December 2017 were recruited for this study. We also enrolled age-matched control subjects and refractive error-matched control subjects among healthy volunteers that visited the hospital for a routine eye examination. The study protocol was approved by the

*Address correspondence. Dr. Mei-Ju Chen, Department of Ophthalmology, Taipei Veterans General Hospital, 201, Section 2, Shih-Pai Road, Taipei 112, Taiwan, ROC. E-mail address: mjchen9069@gmail.com (M.-J. Chen).

Conflicts of interest: The authors declare that they have no conflicts of interest related to the subject matter or materials discussed in this article.

Journal of Chinese Medical Association. (2020) 83: 307-312.

Received May 22, 2019; accepted December 16, 2019.

doi: 10.1097/JCMA.000000000000257.

Copyright © 2020, the Chinese Medical Association. This is an open access article under the CC BY-NC-ND license (<http://creativecommons.org/licenses/by-nc-nd/4.0/>)

institutional review board of our hospital. It was designed in accordance with the Declaration of Helsinki. Written informed consent was obtained from all subjects.

Eyes with focal or diffuse RNFL defects that corresponded to glaucomatous changes in the optic disc and a normal VF test were assigned to the PPG group. Glaucomatous optic disc changes were defined as a vertical CDR >0.7, a difference >0.2 between the CDRs of the glaucomatous eye and its companion eye, and NRR thinning, notching, or excavations observed on optic disc photographs. Focal or diffuse RNFL defects were identified on red-free fundus images. A normal VF was defined as a mean deviation and pattern SD within the 95% confidence limit, and a glaucoma hemifield test result within normal limits, based on a reliable VF test.⁵ A reliable VF test was defined as one with <20% fixation loss, <15% false positives, and <15% false negatives.

All subjects underwent a comprehensive ophthalmic examination. This examination included an assessment of the best-corrected visual acuity, automated refraction and keratometry, Goldman applanation tonometry, a slit-lamp examination, gonioscopy, a dilated fundus exam, red-free fundus photography, and an automated VF examination (Humphrey 24-2 SITA standard algorithm). Eligible subjects met the following inclusion criteria: age ≥20 years, best-corrected visual acuity ≥20/40, open-angle structure based on gonioscopic examination, and astigmatism ≤3 diopters. Control subjects were required to have a normal anterior segment, based on a slit-lamp examination, no glaucomatous changes in the ONH, and a normal VF. Eyes were excluded when they had optic disc areas smaller than 1.56 mm² or larger than 2.30 mm², based on OCT measurements (derived from a mean optic disc area of 1.93 ± 0.37 mm², in 466 normal Chinese subjects)⁶; a severely tilted disc or disc torsion; parapapillary atrophy larger than one disc diameter); any retinal or neurologic disease; ocular inflammation; prior ocular surgery within 3 months; prior refractive surgery or any concurrent disease that could interfere with intraocular pressure measurements or OCT imaging or cause VF defects.

OCT was performed with a Cirrus HD-OCT (Carl Zeiss Meditec) after pupillary dilation. The Cirrus HD-OCT Optic Disc Cube 200 × 200 protocol was used to measure the ONH rim area, disc area, average CDR, vertical CDR, cup volume, average circumferential RNFL (cpRNFL) thickness, and cpRNFL thickness, in quadrants and in 12 clock-hour sectors. The Macular Cube 200 × 200 protocol was used to calculate the average, minimum, and regional macular ganglion cell-inner plexiform layer (GCIPL) thicknesses in six wedge-shaped sectors. The software could also automatically identify the optic disc margin, the cup margin, and the rim area between the disc margin and the cup margin. It then generated a curve composed of points of circumferential rim thickness at each degree (total 360 points). NRR thicknesses were

obtained at intervals of 30° (30°, 60°, 90°, 120°, 150°, 180°, 210°, 240°, 270°, 300°, 330°, and 360°) (Fig. 1). The measurements were labeled in the clockwise direction. For example, in the right eye, the point at 0° (exact temporal point) was labeled 9 o'clock (Fig. 1).

2.1. Statistical analyses

For subjects with two evaluable eyes, the right eye was elected. We analyzed differences between the PPG and normal groups with the Student's *t* test. To evaluate the ability of each parameter to discriminate between PPG and normal eyes, we calculated the area under the receiver operating characteristic curve (AUROC), determined cutoff values, and derived the sensitivities at specificities of 90% and 95% for each parameter. The diagnostic performance was quantified with AUROC values. These values were compared between groups with methods described by DeLong et al.⁷ *p* values 0.05 were considered statistically significant. Statistical analyses were performed with SPSS version 19.0.0 (SPSS, Inc., Chicago, IL).

3. RESULTS

This study included 39 eyes of 39 patients with PPG and 39 eyes of 39 age-matched normal controls and refractive error-matched normal controls. The demographic and clinical characteristics of the subjects are summarized in Table 1. There were no significant between-group differences in age, sex, spherical equivalence, mean deviation, pattern SD, or VF index (VFI). Compared with control eyes, PPG eyes had significantly larger average CDR, vertical CDR, and cup volumes. PPG eyes also had significantly smaller rim areas and NRR thicknesses in corresponding clock-hour sectors (Table 2). Moreover, all GCIPL thicknesses, most cpRNFL thicknesses (except for counterparts in the nasal and temporal quadrant), and some clock-hour RNFL thicknesses (including the 1, 5, 6, 7, 11, and 12 clock-hour sectors) were significantly lower in PPG eyes than in normal eyes (Table 3). Table 4 shows the AUROC values for all OCT parameters. The NRR thickness at 6 o'clock had the largest AUROC value (0.823), followed by the inferior RNFL thickness (0.821), the average RNFL thickness (0.819), the NRR thickness at 7 o'clock (0.818), and the RNFL thickness at 7 o'clock (0.808) (Fig. 2). Comparable diagnostic performances were observed in the NRR thickness at 6 o'clock, the inferior RNFL thickness (*p* = 0.98), the minimum GCIPL thickness (*p* = 0.81), and the rim area (*p* = 0.75), based on AUROC values. Table 5 shows the sensitivities at fixed specificities and the cutoff values of all OCT parameters. At 90% specificity, the rim area had the highest sensitivity (64.1%), followed by the NRR thicknesses at 1 and 2 o'clock (both 61.5%), and the RNFL thicknesses in the superior quadrant and at 6 o'clock (both 53.8%).

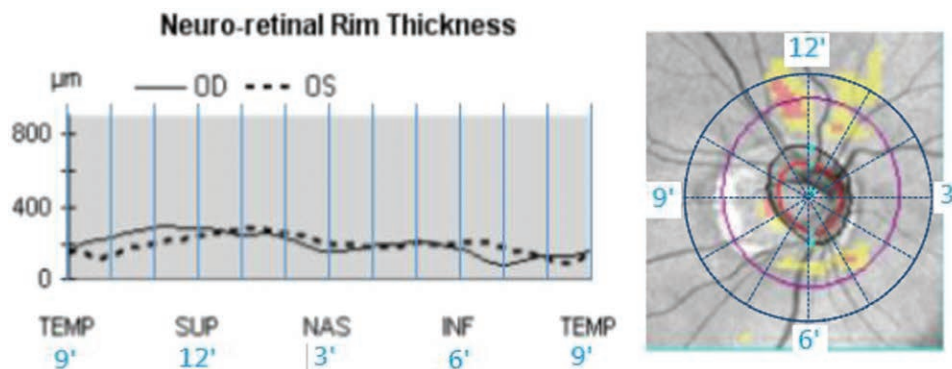


Fig. 1. Points of neuroretinal rim. INF = Inferior; NAS = Nasal; OD = Right eye; OS = Left eye; SUP = Superior; TEMP = Temporal.

Table 1

Demographic and clinical characteristics of the study population

	Normal	PPG	p
Years of age	53.6 ± 16.2	56.4 ± 11.1	0.39
SE (D)	-1.73 ± 2.26	-2.61 ± 1.75	0.06
IOP (mmHg)	17.5 ± 3.4	17.4 ± 3.3	0.84
MD (dB)	-0.94 ± 1.73	-0.96 ± 1.50	0.97
PSD (dB)	1.89 ± 0.95	1.83 ± 0.60	0.72
VFI (%)	98.8 ± 1.61	98.2 ± 2.88	0.22

D = diopter; IOP = intraocular pressure; MD = mean deviation; PPG = preperimetric glaucoma; PSD = pattern standard deviation; SE = spherical equivalent; VFI = visual field index.

Table 2

Comparison of ONH parameters and NRR in clock-hour sectors between two groups

Parameters	Normal	PPG	p
ONH			
Rim area (mm ²)	1.28 ± 0.21	1.04 ± 0.21	<0.001
Disc area (mm ²)	1.91 ± 0.35	1.93 ± 0.31	0.72
Average CDR	0.56 ± 0.21	0.65 ± 0.11	0.02
Vertical CDR	0.49 ± 0.15	0.63 ± 0.12	<0.001
Cup volume (mm ³)	0.18 ± 0.13	0.35 ± 0.23	<0.001
NRR thickness (µm) in clock-hour sectors			
12	370.6 ± 98.2	283.5 ± 92.8	<0.001
1	392.3 ± 111.7	280.8 ± 125.7	<0.001
2	384.3 ± 127.7	291.7 ± 139.7	<0.001
3	390.1 ± 159.3	280.7 ± 128.7	<0.001
4	418.2 ± 148.9	310.6 ± 122.2	<0.001
5	428.9 ± 122.3	326.0 ± 114.2	<0.001
6	417.1 ± 86.0	310.7 ± 77.2	<0.001
7	330.7 ± 98.5	233.7 ± 65.0	<0.001
8	253.2 ± 112.0	184.3 ± 57.1	<0.001
9	231.4 ± 110.6	180.9 ± 56.1	<0.001
10	253.3 ± 107.6	192.9 ± 58.4	<0.001
11	314.1 ± 103.8	235.7 ± 72.5	<0.001

CDR = cup-to-disc ratio; NRR = neuroretinal rim; ONH = optic nerve head; PPG = preperimetric glaucoma.

4. DISCUSSION

In PPG eyes, the largest AUROCs were observed for the NRR thickness at 6 o'clock, the inferior RNFL thickness, the average RNFL thickness, and the NRR thickness at 7 o'clock. The ability of the NRR clock-hour thickness to differentiate between PPG and controls was similar to those of the traditional ONH, RNFL, and GCIPL parameters. In addition, the highest diagnostic performance levels were comparable for the ONH, RNFL, and GCIPL parameters. Many previous studies have compared the performance of different OCT parameters in diagnosing PPG. However, the results have been inconsistent. Begum et al⁸ showed that the ONH and RNFL parameters had significantly higher diagnostic abilities than the GCIPL parameters. In contrast, Seol et al⁹ reported that the diagnostic performance of the minimum GCIPL thickness was superior to those of the RNFL thickness and the rim area. These discrepancies might be explained by the fact that OCT measures a limited scan area of the macular GCIPL; thus, the likelihood of detecting any retinal ganglion cell damaged outside the elliptical annulus is rather low. However, the diagnostic ability of GCIPL parameters increases significantly when the RNFL defects are closer to the fovea.¹⁰ Superotemporal and inferotemporal RNFL bundles tend to converge temporally with increasing myopia.¹¹ In the present study, we found

Table 3

Comparison of cpRNFL and GCIPL parameters between two groups

Parameters	Normal	PPG	p
cpRNFL thickness (µm)			
Average	97.4 ± 8.8	86.2 ± 8.2	<0.001
Superior	118.0 ± 13.9	102.0 ± 14.0	<0.001
Nasal	70.8 ± 10.0	67.6 ± 11.3	0.20
Inferior	123.2 ± 16.9	103.2 ± 14.1	<0.001
Temporal	77.5 ± 14.1	71.5 ± 14.9	0.07
cpRNFL thickness (µm) in clock-hour sectors			
12	116.6 ± 25.0	94.4 ± 23.8	<0.001
1	100.3 ± 21.3	89.6 ± 16.2	0.02
2	81.4 ± 13.0	74.7 ± 17.0	0.06
3	65.3 ± 13.5	65.3 ± 12.3	0.99
4	66.0 ± 13.2	62.7 ± 11.3	0.25
5	92.2 ± 21.7	80.7 ± 15.6	0.01
6	127.9 ± 25.3	105.5 ± 23.9	<0.001
7	149.7 ± 22.3	123.4 ± 19.9	<0.001
8	81.4 ± 19.3	73.7 ± 15.8	0.06
9	60.2 ± 10.7	59.0 ± 11.5	0.64
10	91.0 ± 19.2	83.4 ± 23.3	0.21
11	137.1 ± 18.9	121.7 ± 22.3	<0.001
GCIPL thickness (µm)			
Average	81.4 ± 7.3	76.2 ± 5.0	<0.001
Minimum	78.2 ± 11.1	70.4 ± 7.8	<0.001
Superonasal	85.4 ± 6.42	80.6 ± 7.0	<0.001
Superior	82.1 ± 6.6	77.4 ± 6.4	<0.001
Superotemporal	79.2 ± 10.3	75.3 ± 6.4	0.04
Inferotemporal	80.4 ± 10.9	73.6 ± 7.3	<0.001
Inferior	78.4 ± 9.6	72.4 ± 6.9	<0.001
Inferonasal	83.1 ± 6.8	78.2 ± 6.1	<0.001

cpRNFL = circumpapillary retinal nerve fiber layer; GCIPL = ganglion cell-inner plexiform layer; PPG = preperimetric glaucoma.

comparable diagnostic ability between the GCIPL and RNFL thicknesses. Given the fact that our patients had a relatively low mean refractive error (-2.0 diopter), we speculated that the topographic characteristics (angular location) of the RNFL defects were less affected by myopia, compared with patients with higher degrees of myopia.

In diagnostic ability, Sung et al³ and Lisboa et al¹² reported that the RNFL parameters performed better than ONH measurements did in detecting preperimetric glaucomatous damage; in contrast, our study showed comparable performances between the ONH and RNFL parameters. This difference might be explained by the following observations. First, the diagnostic performance of OCT parameters may be directly related to the definition of PPG. These patients were initially chosen based on a suspicious, glaucomatous appearance of the optic disc, such as enlarged disc cupping or NRR thinning. The RNFL defects were based on red-free fundus images. However, a glaucomatous disc change is more likely to be detected than RNFL thinning during clinical practice. In this setting, the RNFL measurements may not perform better than the ONH assessments. Second, the selection of control eyes may affect the diagnostic performance of OCT parameters. For most OCT parameters, the ability to detect glaucoma decreases significantly when compared with a clinically relevant control group with optic discs that appeared glaucoma suspected.¹³ Conversely, in our control eyes, the inclusion criteria were normal eyes without glaucomatous changes in the optic nerve; thus, the ONH parameters were more readily differentiated between PPG and normal control eyes. Third, the performance of ONH parameters is partly dependent on the morphology of the optic disc. Compared with

Table 4
AUROC, sensitivity at fixed specificity, and cutoff values for ONH and NRR parameters

Parameters	AUROC	Sensitivity at 90% specificity (%)	Cutoff value ^a	Sensitivity at 95% specificity (%)	Cutoff value ^b
ONH					
Rim area	0.801	64.1	1.03	38.5	0.97
Disc area	0.556	10.3	2.24	<0.1	2.81
Average C/D	0.744	48.7	0.69	46.2	0.70
Vertical C/D	0.772	48.7	0.67	41.0	0.68
Cup volume	0.736	43.6	0.37	35.9	0.41
NRR thickness in clock-hour					
12	0.746	43.6	252.5	35.9	242.5
1	0.781	61.5	285.0	61.5	279.0
2	0.749	61.5	263.5	61.5	257.0
3	0.724	48.7	243.5	38.5	229.0
4	0.726	41.0	262.5	35.9	256.5
5	0.752	41.0	283.5	28.2	265.5
6	0.823	48.7	303.0	35.9	281.0
7	0.818	46.2	228.5	35.9	207.5
8	0.743	28.2	154.0	17.9	137.5
9	0.650	23.1	137.0	10.3	111.0
10	0.693	23.1	149.0	10.3	129.0
11	0.737	41.0	209.5	20.5	183.5

AUROC = area under the receiver operating characteristic curves; C/D = cup-to-disc ratio; NRR = neuroretinal rim; ONH = optic nerve head.

^aBased on 90% specificity.

^bBased on 95% specificity.

RNFL measurements, ONH parameters are more susceptible to the influence of individual variability. In the present study, we included only eyes with optic disc areas of 1.56 to 2.30 mm² (derived from the mean optic disc area of 466 normal Chinese subjects).⁶ This criterion reduced the effect of phenotypic optic disc variations on the ONH parameters.

The traditional ONH parameters comprise the disc area, the vertical CDR, the average CDR, the cup volume, and the global rim area. Compared to studies focused on traditional ONH parameters measured with Cirrus HD-OCT,^{2,3} few studies have

focused on the diagnostic ability of NRR thickness in clock-hour sectors. However, to the best of our knowledge, the present study is the first one to evaluate the diagnostic ability of NRR thicknesses in clock-hour sectors for PPG. We found that NRR thicknesses at the 6 and 7 o'clock positions exhibited the largest AUROC values, similar to the findings of Hwang and Kim, who showed that the NRR thicknesses at the 5 and 6 o'clock positions performed best.

Despite the differences between the preperimetric and mild glaucoma stages, the glaucomatous change in the ONH is most evident in the inferior part of the NRR. As glaucoma progresses, the NRR area continuously diminishes. Jonas et al¹⁴ reported that NRR loss occurred in all sectors of the optic disc, and the affected region depended on the stage of the disease. Lloyd et al found that the inferotemporal quadrant was the most common location for glaucoma progression, based on disc photographs.¹⁵ Similarly, the present study showed that the NRR thickness at 6 o'clock was the best indicator of glaucomatous optic disc changes, even in the preperimetric stage. Therefore, the clock-hour NRR assessment appeared to be a valuable method for diagnosing PPG.

This study had several limitations. First, the sample size was relatively small. Second, the ethnicity of all study subjects was Chinese, and therefore, the results might not necessarily be extrapolated to patients of other ethnicities. Third, the definition of PPG was unique to this study. The enrollment criteria could not ensure that all participants had PPG; only a prospective follow-up study would provide sufficient evidence for the diagnosis. Moreover, due to the cross-sectional observation design of this study, no distinct evidence of progression was observed that could differentiate true PPG from suspected glaucoma. Fourth, we assumed that our patients had PPG, based on glaucomatous structural changes and normal VF findings, defined as a normal hemifield test that was symmetric around the horizontal meridian. This definition could have excluded glaucomatous eyes with very early symmetric functional changes, and thus the diagnostic ability of the OCT parameters might have been overestimated. Finally, we did not consider the influence of test-retest variability

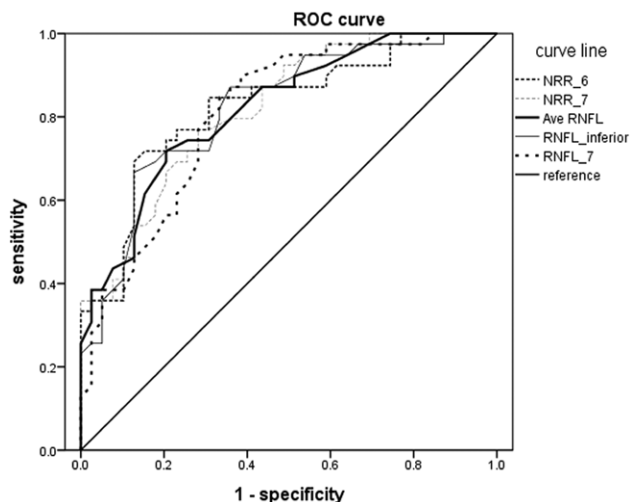


Fig. 2. ROC curve with top five AUROC value. The best parameters for discriminating normal eyes from glaucomatous eyes were the NRR at 6 o'clock (0.823), inferior RNFL thickness (0.821), average RNFL thickness (0.819), NRR at 7 o'clock (0.818), and RNFL thickness in sector at 7 o'clock (0.808). AUROC = area under the receiver operating characteristics curve; NRR = neuroretinal rim; RNFL = retinal nerve fiber layer; ROC = receiver operating characteristics.

Table 5
AUROC, sensitivity at fixed specificity, and cutoff values for cpRNFL and GCIPL parameters

Parameters	AUROC	Sensitivity at 90% specificity (%)	Cutoff value ^a	Sensitivity at 95% specificity (%)	Cutoff value ^b
cpRNFL thickness (μm)					
Average	0.819	43.6	85.5	38.5	84.5
Superior	0.783	53.8	102	53.8	100.5
Nasal	0.606	15.4	58.5	10.3	53.5
Inferior	0.821	43.6	103.5	35.9	99.5
Temporal	0.643	23.1	61.5	17.9	58
cpRNFL thickness (μm) in clock-hour sectors					
12	0.746	51.3	92.5	43.6	84.5
1	0.651	17.9	73.0	10.3	66.0
2	0.643	43.6	68.5	41.0	66.0
3	0.500	7.7	49.0	2.6	42.0
4	0.575	10.3	50.5	5.1	46.5
5	0.671	33.3	70.5	25.6	68.5
6	0.758	53.8	102.5	28.2	93.5
7	0.808	38.5	121.0	38.5	119.5
8	0.619	17.9	58.5	12.8	56.5
9	0.534	15.4	48.0	5.1	43.5
10	0.606	28.2	71.0	28.2	68.5
11	0.689	38.5	113.5	30.8	108.5
GCIPL thickness (μm)					
Average	0.745	20.5	72.5	15.4	71.5
Minimum	0.807	48.7	71.5	38.5	68.5
Superonasal	0.688	25.6	76.5	15.4	74.5
Superior	0.699	20.5	73.5	15.4	70.5
Superotemporal	0.698	23.1	70.5	12.8	68.5
Inferotemporal	0.776	46.2	73.5	38.5	72.5
Inferior	0.751	43.6	71.5	25.6	69.5
Inferonasal	0.698	33.3	75.5	15.4	71.5

AUROC = area under the receiver operating characteristic curves; cpRNFL = circumferential retinal nerve fiber layer; GCIPL = ganglion cell–inner plexiform layer.

^aBased on 90% specificity.

^bBased on 95% specificity.

on the OCT analysis. The performance of the built-in software algorithm provided with the HD-OCT might have affected the results. Despite these limitations, this study demonstrated several effective parameters for discriminating between PPG and normal eyes in clinical practice. In addition, we showed that the NRR measurements could be readily obtained without any special image-processing software. Our results indicated that the clock-hour NRR assessment was useful for the early detection of glaucoma.

In conclusion, in the present study, we used spectral-domain OCT to evaluate the ability of clock-hour NRR measurements to diagnose PPG in patients. Our results showed that the ability of NRR thickness measurements to diagnose PPG was comparable to that of traditional ONH, RNFL, and GCIPL analyses. The NRR thickness at the 6 o'clock position showed superior performance compared with all other parameters tested. Thus, this parameter could play a role in detecting early structural changes in PPG.

REFERENCES

- Mwanza JC, Chang RT, Budenz DL, Durbin MK, Gendy MG, Shi W, et al. Reproducibility of peripapillary retinal nerve fiber layer thickness and optic nerve head parameters measured with cirrus HD-OCT in glaucomatous eyes. *Invest Ophthalmol Vis Sci* 2010;51:5724–30.
- Mwanza JC, Oakley JD, Budenz DL, Anderson DR; Cirrus Optical Coherence Tomography Normative Database Study Group. Ability of cirrus HD-OCT optic nerve head parameters to discriminate normal from glaucomatous eyes. *Ophthalmology* 2011;118:241–8.e1.
- Sung KR, Na JH, Lee Y. Glaucoma diagnostic capabilities of optic nerve head parameters as determined by Cirrus HD optical coherence tomography. *J Glaucoma* 2012;21:498–504.
- Hwang YH, Kim YY. Glaucoma diagnostic ability of quadrant and clock-hour neuroretinal rim assessment using cirrus HD optical coherence tomography. *Invest Ophthalmol Vis Sci* 2012;53:2226–34.
- Budenz DL. *Atlas of visual fields*. Philadelphia, PA: Lippincott-Raven, 1997;143–5.
- Tun TA, Sun CH, Baskaran M, Girard MJ, de Leon JM, Cheng CY, et al. Determinants of optical coherence tomography-derived minimum neuroretinal rim width in a normal Chinese population. *Invest Ophthalmol Vis Sci* 2015;56:3337–44.
- DeLong ER, DeLong DM, Clarke-Pearson DL. Comparing the areas under two or more correlated receiver operating characteristic curves: a nonparametric approach. *Biometrics* 1988;44:837–45.
- Begum VU, Addepalli UK, Yadav RK, Shankar K, Senthil S, Garudadri CS, et al. Ganglion cell-inner plexiform layer thickness of high definition optical coherence tomography in perimetric and preperimetric glaucoma. *Invest Ophthalmol Vis Sci* 2014;55:4768–75.
- Seol BR, Jeoung JW, Park KH. Glaucoma detection ability of macular ganglion cell-inner plexiform layer thickness in myopic preperimetric glaucoma. *Invest Ophthalmol Vis Sci* 2015;56:8306–13.
- Kim MJ, Jeoung JW, Park KH, Choi YJ, Kim DM. Topographic profiles of retinal nerve fiber layer defects affect the diagnostic performance of macular scans in preperimetric glaucoma. *Invest Ophthalmol Vis Sci* 2014;55:2079–87.
- Leung CK, Yu M, Weinreb RN, Mak HK, Lai G, Ye C, et al. Retinal nerve fiber layer imaging with spectral-domain optical coherence tomography: interpreting the RNFL maps in healthy myopic eyes. *Invest Ophthalmol Vis Sci* 2012;53:7194–200.
- Lisboa R, Paranhos A Jr, Weinreb RN, Zangwill LM, Leite MT, Medeiros FA. Comparison of different spectral domain OCT scanning

- protocols for diagnosing preperimetric glaucoma. *Invest Ophthalmol Vis Sci* 2013;54:3417–25.
13. Rao HL, Kumbar T, Addepalli UK, Bharti N, Senthil S, Choudhari NS, et al. Effect of spectrum bias on the diagnostic accuracy of spectral-domain optical coherence tomography in glaucoma. *Invest Ophthalmol Vis Sci* 2012;53:1058–65.
 14. Jonas JB, Fernández MC, Stürmer J. Pattern of glaucomatous neuroretinal rim loss. *Ophthalmology* 1993;100:63–8.
 15. Lloyd MJ, Mansberger SL, Fortune BA, Nguyen H, Torres R, Demirel S, et al. Features of optic disc progression in patients with ocular hypertension and early glaucoma. *J Glaucoma* 2013;22:343–8.